Title
Rate effects on the undrained shear strength of compacted clay

Journal
Soils and Foundations, 56(4)

ISSN
0385-1621

Authors
Mun, W
Teixeira, T
Balci, MC
et al.

Publication Date
2016-08-01

DOI
10.1016/j.sandf.2016.07.012

Peer reviewed

Manuscript

RATE EFFECTS ON THE UNDRAINED SHEAR STRENGTH OF COMPACTED CLAY

By W. Mun, Ph.D.[1], T. Teixeira, B.S.[2], M.C. Balci, M.S.[3], J. Svoboda, M.S.[4], and J.S. McCartney, Ph.D., P.E.[5]

Abstract: Unconsolidated-undrained (UU) triaxial compression tests were performed on low-plasticity clay specimens compacted to the same void ratio but different initial degrees of saturation to evaluate the impact of axial strain rates ranging from 0.1 to 150 %/min on the undrained shear strength. Although an effective stress analysis cannot be performed on the results, they are useful to evaluate the relative roles of initial hydraulic conditions (i.e., matric suction and degree of saturation) and compaction effects (i.e., potential changes in soil structure with compaction water content). This evaluation is relevant due to difficulty in measuring shear-induced pore water and air pressures in consolidated-undrained (CU) compression tests on unsaturated clay. In all tests, the undrained shear strength quantified as the maximum principal stress difference increased log-linearly with axial strain rate, with rates of increase ranging from 4.1 to 9.7% per log cycle of axial strain rate for specimens having initial degrees of saturation ranging from 0.99 to 0.59. The undrained shear strength, rate of increase in undrained shear strength with axial strain rate, and secant moduli all increased nonlinearly with decreasing initial degree of saturation, although compaction effects played an important role in these trends. The increase in undrained shear strength with axial strain rate can be attributed to a reduction in the magnitude of excess pore water pressure, with similar reductions in magnitude for all the degrees of saturation considered. A comparison between the measured undrained shear strength values

[1] Research Associate, Dept. of Structural Eng., Univ. of California San Diego, 9500 Gilman Dr., La Jolla, CA 92093-0085
[2] Undergrad. Student, Dept. of Civil, Env. and Arch. Eng. Univ. of Colorado Boulder, UCB 428, Boulder, CO 80309
[3] Doctoral Candidate, Batman University, Batman, Turkey
[4] Engineer, Jackola Eng. and Arch., Kalispell, MT
[5] Associate Professor, Dept. of Structural Eng., Univ. of California San Diego, 9500 Gilman Dr., La Jolla, CA 92093-0085

and the drained shear strength values estimated using the suction stress concept was useful in delineating the impacts of initial hydraulic conditions and compaction effects on the trends in measured undrained shear strength.

INTRODUCTION

There are many situations in geotechnical engineering systems where the loading rate may be substantially greater than those employed in standard laboratory tests used to obtain shear strength properties, including impact loading, blast loading, wave loading, or earthquake loading. It is well established that the undrained shear strength of saturated clays increases log-linearly with the axial strain rate due to lower magnitudes of excess pore water pressure generation during faster tests. However, the impacts of loading rate on the undrained shear strength of unsaturated soils may be more complicated than in saturated soils due to the effects of matric suction and degree of saturation on the stress state, effects of compaction, generation of shear-induced excess pore air and water pressures, hydraulic hysteresis, and lower hydraulic conductivity than in saturated conditions. While considerable research has been focused on the shear strength of unsaturated soils in terms of both experimental characterization (Fredlund et al. 1978; Ho and Fredlund 1982; Escario and Saez 1986; Rahardjo et al. 1995; Feuerharmel et al. 2005; Nam et al. 2011) and predictive models (Fredlund et al. 1987; Abramento and Carvalho 1989; Vanapalli et al. 1996), fewer studies have focused on investigating the role of unsaturated conditions on the undrained shear strength of unsaturated, compacted clays subject to elevated strain rates (Olson and Parola 1967; Svoboda and McCartney 2014).

The behavior of compacted soils sheared at different rates is important as the initial degree of saturation may influence the undrained shear strength through changes in the initial effective stress state (Bishop 1959) and the potential magnitudes of excess pore air and pore water pressures generated during shear (Hilf 1948). However, consolidated-undrained (CU) or constant water content (CW) tests on unsaturated soils are time consuming, and measurements of excess pore water pressure at the boundary of unsaturated soil specimens in these tests may not be representative of those near the shear plane. Accordingly, the goal of this study is to assess the role of elevated axial strain rates on the undrained shear strength of unsaturated, compacted clay specimens obtained from unconsolidated-undrained (UU) triaxial compression tests. Although these UU tests do not permit the evaluation of shear-induced excess pore water pressures, they allow for examination of the relative roles of the initial hydraulic conditions (i.e., the initial matric suction and degree of saturation) and compaction effects (i.e., potential changes in soil structure when a soil is compacted wet or dry of optimum) on the undrained shear strength. Further, UU triaxial compression tests can be performed in a short period of time to facilitate characterization of variability in undrained shear strength. Furthermore, the air and water drainage conditions in a UU test also represent the pore fluid drainage conditions expected during rapid loading.

Compaction is expected to have complex effects on the undrained shear strength of unsaturated soils. Olson and Langfelder (1965) found that compaction of soils at different gravimetric water contents will lead to a variation in the initial suction, while Mitchell et al. (1965) found that compaction of clays will lead to a change in behavior from that associated with a flocculated structure to that associated with a dispersed structure as the compaction water content passed from being dry of optimum to wet of optimum. The initial suction and degree of saturation in the specimen may affect the effective stress and thus the shear strength (Bolzon and Schrefler 1998; Lu et al. 2010), while Mitchell et al. (1965) found that the shear strength and hydraulic conductivity were higher for flocculated specimens compacted dry of optimum than for dispersed specimens compacted wet of optimum. Mitchell et al. (1965) hypothesized that flocculated specimens have greater interlocking between particles while dispersed specimens have particles aligning parallel to each other. Although changes in compaction-induced soil structure were not experimentally verified in this study, the effect of soil structure on soil behavior and in particular the undrained shear strength has been well established in the technical literature (Mitchell et al. 1965; Seed and Chan 1959; Vanapalli et al. 1999; Cetin and Gökoğlu 2013). Accordingly, the potential changes in soil structure for specimens compacted or dry of optimum are referred to simply as compaction effects in this study, while the degree of saturation and matric suction were determined independently.

This study involved the evaluation of the undrained shear strength of compacted clay specimens prepared at the same initial void ratio but different initial degrees of saturation. Assuming that the optimum water content occurs at a degree of saturation of 0.9 for a given compaction water content, initial degrees of saturation of 0.99 and 0.90 were selected to represent the behavior of soils compacted wet of optimum, while initial degrees of saturation of 0.70 and 0.60 were selected to represent the behavior of soils compacted dry of optimum. To assess the impact of the initial hydraulic conditions, the suction stress concept of Lu et al. (2010) was employed to estimate the impact of suction on the shear strength of the clay specimens under drained conditions. A comparison between drained and undrained shear strength values permits assessment of the relative effects of initial hydraulic conditions (and associated effective stress state), the potential for shear-induced excess pore water pressure generation, as well as compaction effects.

BACKGROUND

Most studies on strain rate effects on shearing behavior of saturated clay have employed quasi-static triaxial compression tests under strain-controlled conditions, potentially with either pore water pressure measurements, or impulse loading compression tests which were under stress-controlled conditions. As most low-permeability soils will not have sufficient time for drainage during fast shearing, most studies have focused on understanding axial strain rate effects on the undrained shear strength. A summary of the results from several studies on the impact of axial strain rates on the undrained shear strength of saturated and unsaturated clay specimens having different mineralogies, stress states, and stress histories is presented in Table 1. Although Olson and Parola (1967) found that there may be more curvature in the relationship between undrained shear strength and the rate of loading at very high axial strain rates (i.e., greater than 1000 %/min), most of the studies summarized in Table 1 reported that most clay soils experience an average increase in undrained shear strength of 10% per log cycle of axial strain rate.

Most researchers have hypothesized that rate effects on the undrained shear strength of clays results from changes in the tendency for shear-induced volume change, resulting in lower magnitudes of excess pore water pressures at faster rates. Richardson and Whitman (1963) observed a decrease in the excess pore water pressure measured at the center of a saturated clay specimen sheared under an axial strain rate that was 500 times faster than the rate that would correspond to 90% equalization of pore water pressure, which led to a greater mean effective stress at failure for the faster test. They also observed that shear planes did not tend to form in the specimen until reaching relatively large strains and that pore water pressure was not strain rate dependent at strains less than 0.5%. Other studies have observed that soils become stiffer as the axial strain rate is increased, leading to a smaller axial strain at failure (Casagrande and Shannon 1948; Richardson and Whitman 1963; Olson and Parola 1967; Zhu and Yin 2000). This increase in stiffness with axial strain rate may correspond to the lower tendency to change in volume during shear. This is consistent with the hypothesis of Soga and Mitchell (1996), who assumed that pore water pressure generation is more related to the magnitude of strain rather than the strain rate. The shear strength of dry sands under relatively low confining stresses experience negligible rate effects, indicating that the axial strain rate may not affect the friction angle of soils (Svoboda and McCartney 2013).

Although unsaturated conditions may have an important effect on the shear strength of clays, it is difficult to evaluate rate effects due to challenges in instrumentation, low permeability, and compression of the air phase. Nonetheless, there are several relevant lessons that can be learned from drained and undrained shear strength tests on unsaturated soils under conventional loading rates. Escario and Saez (1986) performed drained shear strength tests on unsaturated soils and observed that the shear strength increases with suction and net normal stress. Lu and Likos (2006) reinterpreted their data in terms of effective stress, and found that there the matric suction does not affect the slope of the failure envelope. Matric suction does affect the shear strength through variations in the stress state (Bishop 1959; Bolzon and Schrefler 1995; Lu et al. 2010), and several experimental studies observed that the variation of shear strength with matric suction is nonlinear (Escario and Saez 1986; Gan et al. 1988; Rassam and Williams 1999; Nam et al. 2011). The soil-water retention curve (SWRC) has been used as a tool in the prediction of the shear strength along with the saturated shear strength parameters (Vanapalli et al. 1996; Vanapalli and Fredlund 2000). Although there are several formulations for quantifying the effects of matric suction on the effective stress state and the shear strength of unsaturated soils, Bolzon and Schrefler (1995) and Lu et al. (2010) developed linkages between the effective stress and SWRC models.

Olson and Parola (1967) performed one of the few studies on the impact of strain rate on the undrained shear strength of unsaturated, compacted soils. They performed UU triaxial tests on compacted Goose Lake clay at different initial gravimetric water contents at axial strain rates ranging from approximately 0.2 to 4.0×10^5 %/min. For tests at the same strain rate, specimens with the lowest water content had the greatest undrained shear strength at failure. As the compaction water content increased, the undrained shear strength of the clay decreased. However, they only considered the effect of axial strain rate on the undrained shear strength by differentiating between the initial compaction water contents but did not consider the role of initial suction. Further, the specimens had different initial void ratios. Consistent with the observations of Mitchell et al. (1965), they found that soil structure also plays an important role in the rate effects on compacted soils, where the undrained shear strength of soils compacted wet of optimum was much lower than that of soils compacted dry of optimum. Also similar to the observations of Mitchell et al. (1965), Olson and Parola (1967) did not see a significant difference in undrained shear strength with different initial water contents dryer than optimum for tests performed at relatively low confining stresses (690 kPa), indicating that soil structure may play the greatest role in changing soil behavior near the optimal compaction water content. Olson and Parola (1967) also observed that the confining stress used in the unconsolidated undrained shear strength tests at different rates on unsaturated, compacted soils can have a significant impact on the magnitude of undrained shear strength, especially at high confining stresses (6900 kPa), contrary to the role of confining stress in UU tests on water-saturated soils.

Svoboda and McCartney (2014) observed that the undrained shear strength of compacted Boulder clay in both saturated and unsaturated conditions increases log-linearly with increasing strain rate from a series of consolidated-undrained (CU) triaxial compression tests. In their research, the excess pore water pressure at the bottom boundary of the specimen was consistently positive for both the saturated and unsaturated specimens at failure. Cunningham et al. (2003) observed that the pore water pressures measured at a specimen boundary may not be representative of those on the failure plane in unsaturated soils. In particular, this occurs when the pore water phase is not connected across the length of the specimen (i.e., when the soil specimen has a relatively low degree of saturation).

MATERIAL

The soil evaluated in this study was obtained from a stockpile at a construction site on the University of Colorado Boulder campus, and is referred to as Boulder clay. The clay was ground in air-dry conditions then processed to remove all particles with a diameter greater than 2 mm (retained on the #10 sieve), which provided a more homogeneous and consistent material for experimental testing. The processed Boulder clay is classified as a low plasticity clay (CL) according to the Unified Soil Classification System (USCS). Some of the geotechnical characteristics of Boulder clay are listed in Table 2.

The standard Proctor compaction curve for Boulder clay is shown in Figure 1(a), along with the initial compaction points for the different UU test specimens. A compaction water content of 17.5% and a dry unit weight of 17.4 kN/m^3 correspond to optimum conditions for the standard Proctor compaction effort. The shape of the compaction curve supports the assumption that the line of optimums corresponds to a line of constant degree of saturation of 0.9, so the arrows in this figure define which specimens can be considered wet or dry of optimum. As one of the goals of this study is to evaluate the role of the initial suction on rate effects on the undrained shear strength, the initial suction values in several of the compacted specimens having different initial degrees of saturation were assessed using a carefully de-aired UMS T5 tensiometer, with the time series of suction equilibration shown in Figure 1(b). In order to prevent cavitation during suction measurement, the tensiometer was saturated using de-aired water by applying positive pressure of 140 kPa and a negative pressure of 80 kPa before each test. After equilibration of the tensiometer, an increasing initial suction is observed with decreasing initial degree of saturation, as shown in Figure 1(b). The Transient Water Release and Imbibition Method (TRIM) of Wayllace and Lu (2012) was used to infer the drying and wetting paths of the SWRC for a Boulder clay specimen having the same initial void ratio as that used in the undrained triaxial tests (0.52) under unconfined conditions, as shown in Figure 1(c). This approach permitted inverse estimation of the van Genuchten (1980) SWRC model parameters α and n for the drying and wetting paths, which are shown in the figure. The air entry suction for the drying path is approximately 40 kPa. The equilibrium suction-saturation points for the specimens evaluated using the tensiometer in Figure 1(b) are also shown in Figure 1(c), which correspond well with the drying path of the SWRC from the TRIM analysis.

EXPERIMENTAL APPROACH

A series of UU triaxial compression tests was performed on compacted specimens of Boulder clay to investigate the effects of strain rate, initial hydraulic conditions, and compaction effects on the undrained shear strength. Although the tests focused on compacted specimens with varying initial degrees of saturation and different axial strain rates, the general testing procedures followed the standard for UU triaxial compression testing described in ASTM D2850 (ASTM 2007).

The clay specimens were prepared using static compaction with a mechanical loading press to reach the same initial void ratio of 0.52, but with different initial degrees of saturation. Lines of constant degree of saturation are shown in Figure 1(a) to put these initial conditions into perspective with the standard Proctor compaction curve. Each specimen was compacted into a cylindrical mold that is 71.1 mm high with a 35.6 mm diameter. To ensure uniformity throughout the sample, each specimen was compacted using three lifts of equal mass at gravimetric water contents of 11.5, 13.5, 17.5, and 19.5% to reach the same target dry unit weight of 17.4 kN/m^3 (i.e., a target void ratio of 0.52). A conventional triaxial testing setup with no drainage ports in the top and bottom platens was used, and the specimens were encased within a latex membrane. For each of the specimens, a total confining stress of 207 kPa was immediately applied after assembly of the cell without permitting drainage or air or water, after which the specimen was allowed to rest without drainage for a minimum of 10 minutes. This magnitude of confining stress is not expected to lead to pressurized saturation of the specimens based on the results from undrained compression tests on this soil reported by Mun and McCartney (2015). For each set of specimens having a different initial degree of saturation, UU tests were performed at four different axial strain rates under displacement control conditions: 0.1, 1.5, 15.0, and

150.0%/minute, with each combination repeated three times for variability characterization. These axial strain rates correspond to shearing times (i.e., the time required to reach 15% axial strain) of 150, 10, 1 and 0.1 minutes. A motor-driven load frame manufactured by ELE International (model Digital Tritest 50) was used to shear the specimens for displacement rates up to 10 mm/min (axial strain rates less than 15.0 %/min), while a hydraulic press manufactured by Wille Geotechnik (model LO 70XX/DYN-SH) was used for the tests with an axial strain rate of 150 %/min. In both cases, the axial displacement as well as the axial load were monitored independently by using a linearly-variable deformation transformer (LVDT) and the load cell mounted on the cross head of the load frame. All tests for a given strain rate and initial degree of saturation were repeated three times in order to assess variability. The gravimetric water content at failure was measured at the shear plane of the specimen for each test, and were found to be nearly identical to the compaction water content values, confirming a negligible change in water content during shearing in the UU tests. Summaries of the average values of compaction water content, degree of saturation and initial void ratio for the UU tests are listed in Table 3.

EXPERIMENTAL RESULTS

The principal stress difference (σ_1-σ_3), where σ_1 is the major principal total stress equal to the axial stress and σ_3 is the minor principal total stress equal to the cell pressure, is plotted as a function of axial strain for specimens under different water contents and axial strain rates in Figure 2. The curves in this figure are the average of three curves performed under the same conditions, with excellent repeatability observed under each combination. The undrained shear strength in this study is presented in terms of the principal stress difference at failure $(\sigma_1-\sigma_3)_f$, which is equivalent to twice the undrained shear strength. When evaluating the stress-strain curves, the principal stress difference at failure $(\sigma_1-\sigma_3)_f$ was defined as either the maximum value of the principal stress difference from the stress-strain curve in the case that a peak value was observed, or the value of principal stress difference at an axial strain of 15% in the case that no peak value was observed. A summary of the test results is presented in Table 4, which provides all of the values including average values with standard deviations from repeated tests. Regardless of the compaction water content, an increase in $(\sigma_1\text{-}\sigma_3)_f$ with increasing strain rate is observed in the stress strain curves in Figure 3. Further, $(\sigma_1\text{-}\sigma_3)_f$ increases with decreasing compaction water content regardless of the applied strain rate. A transition in the shapes of the stress-strain curves is also observed. The specimens with the two lower compaction water contents show a peak value at an axial of approximately 3-6% followed by strain softening, while the specimens with the two greater compaction water content show strain hardening throughout shearing.

The values of $(\sigma_1\text{-}\sigma_3)_f$ from the UU triaxial tests on specimens compacted at different water contents as a function of the axial strain rate are shown in Figure 3(a). The data points signify the average of the three tests at each testing condition, while the error bars denote the range of the principal stress differences measured in the repeated tests. Consistent with observations from the literature, the results indicate that $(\sigma_1\text{-}\sigma_3)_f$ increases log-linearly with axial strain rate. The following equation was fit to each data set shown in Figure 3(a):

$$(\sigma_1 - \sigma_3)_f = A\log(\dot{\varepsilon}) + B \qquad (1)$$

where $\dot{\varepsilon}$ is the axial strain rate and A and B are the slope and intercept values of the semi-logarithmic relationship, respectively.

The average axial strains at failure corresponding to the points in Figure 3(a) are plotted as a function of axial strain rate in Figure 3(b). Specimens with lower compaction water contents failed at an axial strain less than 15%, with a decrease in the axial strain at failure with increasing axial strain rate. This indicates that stiff soils will behave in an even stiffer manner when sheared at faster rates. The greater strength of the specimens sheared at faster rates supports the hypothesis of Soga and Mitchell (1996) that lower excess pore water pressures may be induced in the specimens that fail at a smaller axial strain. The axial strain at failure is greater for specimens with higher initial water contents. All of the specimens with water contents wet of optimum (17.6 and 19.3%) reached an axial strain of 15% without exhibiting a peak value, irrespective of the axial strain rate.

ANALYSIS

Overview

One of the goals of this study is to discern the relative impacts of the initial hydraulic conditions and compaction effects on the undrained shear strength of compacted clays. The initial values of suction and degree of saturation may affect both the initial effective stress in the specimen, and compaction of specimens wet or dry of optimum may lead to changes in soil behavior. Although it is not possible to evaluate shear-induced excess pore water pressures in the UU tests, the compaction effects may affect the magnitude of excess pore water pressures generated during shearing at different rates due to the relative amounts of each fluid within the soil. Two analyses are performed in this study to investigate the relative effects of other factors affecting undrained shear strength. First, the rate of increase in $(\sigma_1-\sigma_3)_f$ with axial strain rate, the magnitude of $(\sigma_1-\sigma_3)_f$, and the secant modulus are plotted as function of the initial degree of saturation and suction. However, as the trends in these figures may mask the effects of compaction effects, a second analysis is performed to compare the measured undrained shear strength values with the drained shear strength values that would be expected for a similar initial effective stress. This comparison involves the assessment of two expected behaviors: (1) does the increase in undrained shear strength with initial suction follow a similar trend; and (2) is the magnitude of the undrained shear strength less than that of the drained shear strength due to positive excess pore water pressures expected during faster shearing tests (Svoboda and McCartney 2014). Deviations from the expected behaviors may reveal the role of the specimen being compacted wet or dry of optimum. The challenge of this comparison is to select the same initial effective stress for the drained tests, which requires an estimate of the impact of suction on the effective stress and an estimate of the impact of the change air pressure generated by the application of the cell pressure.

Impact of Initial Hydraulic Conditions and Compaction Effects

Although it is clear that the initial suction and degree of saturation have an effect on the undrained shear strength, it is possible that compaction effects may be superimposed on these trends. As the results in Figure 1(b) indicate that the initial suction (ψ_i) values measured using the tensiometer match well with those from the drying-path SWRC, the initial suction values were estimated using the SWRC model of van Genuchten (1980), expressed as follows:

$$\psi = \frac{1}{\alpha}\left\{S_e^{-\frac{n}{n-1}} - 1\right\}^{\frac{1}{n}} \quad (1)$$

where S_e is the effective saturation [i.e., $S_e=(S_r-S_{res})/(1-S_{res})$, where S_r is the degree of saturation and S_{res} is the residual saturation] and α and n are fitting parameters.

The log-linear slopes of the relationship between $(\sigma_1\text{-}\sigma_3)_f$ and axial strain rate (Parameter A from Eq. 1) for each different water content are plotted against initial the degrees of saturation and estimated initial suction in Figures 4(a) and 4(b), respectively. The magnitudes of log-linear slopes increase with decreasing initial degree of saturation and with increasing initial suction. The rate of increase in $(\sigma_1\text{-}\sigma_3)_f$ tends to decay with decreasing degree of saturation, indicating that the amount of pore water plays a role in the rate effects. The values of $(\sigma_1-\sigma_3)_f$ are plotted against the initial degree of saturation and estimated initial suction in Figures 5(a) and 5(b), respectively. An interesting observation from the results in Figure 5 is that the rate effects are similar regardless of the initial degree of saturation (i.e., a uniform shift upward). This indicates that the excess pore air and pore water pressures at different initial degrees of saturation have the same net effect on the effective stress state. The value of $(\sigma_1-\sigma_3)_f$ increases with decreasing initial degree of saturation and increasing initial suction. Although Mitchell et al. (1965) observed that the undrained shear strength was relatively constant for specimens compacted dry of optimum, this may be because their specimens were all prepared using the same compaction effort and had different void ratios as well as initial suction values. It is possible that the effects of compaction wet or dry of optimum and the initial effective stress associated with the initial suction and initial degree of saturation offset in their tests. Although partially due to the log scale, a different trend in the increase in $(\sigma_1-\sigma_3)_f$ with initial suction is observed for the specimens compacted at or less than optimum (i.e., the two lower suction values) than those compacted dry of optimum. The large jump in $(\sigma_1-\sigma_3)_f$ between the two middle suction values is an indicator that the impact of compacting the specimen wet or dry of optimum may be superimposed atop the initial suction effects for specimens compacted to the same void ratio.

Not only is the secant modulus from the stress strain curves linked with the magnitude of the principal stress at failure, but it also may reflect the tendency for volume change during the undrained tests. The average secant modulus at an axial strain of 1% as a function of the axial strain rate for specimens with different initial hydraulic conditions is shown in Figure 6, along with the error bars. The secant modulus clearly increases with axial strain rate, albeit with a greater rate of increase for the specimens compacted dry of optimum. The average secant modulus was plotted as a function of the initial degree of saturation and estimated initial suction in Figures 7(a) and 7(b), respectively. Similar to the trends observed for $(\sigma_1-\sigma_3)_f$, the secant modulus increases with decreasing initial degree of saturation and increasing initial suction. Although a relatively uniform upward shift with axial strain was observed in the data regardless of the initial degree of saturation, a significant upward shift in secant modulus was observed for the fastest axial strain rate. Similar increases in the secant modulus with decreasing compaction water content were observed by Olson and Parola (1967).

Comparison of Undrained and Drained Shear Strength Values

As mentioned, the difference between the undrained and drained shear strength values is expected to reflect the magnitude of excess pore water pressure conditions, the impact of suction on the shear strength, and the role of compaction effects. The shear strength of soil under drained conditions, quantified using the maximum principal stress difference $(\sigma_1-\sigma_3)_f$, can be estimated from the Mohr-Coulomb failure criterion, as follows:

$$(\sigma_1 - \sigma_3)_f = \frac{2\sigma_3'\sin\phi'}{1-\sin\phi'} \qquad (3)$$

where ϕ' is the friction angle (assumed to be constant with suction), and σ_3' is the effective minor principal stress equal to the effective confining stress. The effective stress can be estimated using the effective stress definition of Bishop (1959), given as follows:

$$\sigma' = (\sigma - u_a) + \chi(u_a - u_w) \qquad (4)$$

where the difference between total stress σ and the pore-air pressure u_a is referred to as the net stress σ_{net}, and χ is the effective stress parameter. Lu and Likos (2006) hypothesized that the term $\chi(u_a-u_w)$ could be replaced by the suction stress σ_s to up-scale the effects of capillarity and other inter-particle forces that may vary with degree of saturation or suction, as follows:

$$\sigma' = (\sigma - u_a) - \sigma_s \quad (5)$$

Lu et al. (2010) referred to the functional relationship between suction stress and suction for a given soil under a certain stress state as the suction stress characteristic curve (SSCC). In order to define the SSCC, Lu et al. (2010) made a similar assumption to Bolzon and Schrefler (1995) that the effective stress parameter in Equation (4) is equal to the effective saturation S_e, which permits a SWRC model such that that of van Genuchten (1980) to be incorporated into the definition of σ_s as follows:

$$\sigma_s = -\frac{S_e}{\alpha}\left\{S_e^{\frac{n}{n-1}} - 1\right\}^{\frac{1}{n}} \quad (6)$$

The drying path SWRC for Boulder clay along with the SSCC estimated using Equation (6) are shown in Figure 8(a). Consistent with the silty soil evaluated by Lu et al. (2010) and for soils with a van Genuchten (1980) SWRC when n parameter is greater than 2.5, the SSCC exhibits a peak value at a mid-range of suction. This indicates that suction has an optimal effect on the effective stress at mid-range values of effective saturation.

One of the challenges in applying Equation (5) in a comparison between the drained and undrained shear strength values is the selection of the air pressure to use in the definition of the net stress (σ-u_a). This may be obtained using the pore pressure analysis of Hilf (1948), who combined Boyle's law and a simplified form of Henry's law to estimate the change in pore air pressure expectation during changes in porosity of unsaturated soils under undrained conditions. He assumed that the matric suction does not significantly change during undrained compression, which was later confirmed by Bishop and Donald (1961) and Rahardjo (1990). In this case, the change in pore air pressure (Δu_a) is equal to the change in pore water pressure (Δu_w). Considering the volumetric strain of the unsaturated soil under undrained compression [i.e.,

$\Delta n = m_v(\Delta p - \Delta u_a)$], the change in pore air pressure (Δu_a) with a change in total cell pressure ($\Delta\sigma_3$) can be expresses as follows:

$$\Delta u_a = \left[\frac{1}{1 + \frac{(1 - S_{r,0} + hS_{r,0})n_0}{(u_{a0} + \Delta u_a)m_v}} \right] \Delta\sigma_3 \quad (7)$$

where $S_{r,0}$ is the initial degree of saturation, n_0 is the initial porosity, h is the volumetric coefficient of solubility assumed to be 0.02, u_{a0} is the initial absolute pore-air pressure which assumed to be atmospheric (i.e., 101.3 kPa), and m_v is the coefficient of volume compressibility of soil obtained from undrained compression tests on this clay performed by Mun and McCartney (2015). An iterative approach is needed to solve for the change in air pressure (Δu_a) to satisfy Equation (7) because the unknown term (Δu_a) appears on both sides of the equation. The relationship between pore-air pressure and total stress estimated by using Equation (7) using the input values summarized in Table 5 is shown in Figure 8(b). For the change in total stress during application of the cell pressure (207 kPa), the difference in the change in pore air pressure was not significant for the specimens having different initial degrees of saturation. For simplicity, an average change in pore air pressure of 6.3 kPa was incorporated in Equation (5) to define the initial effective stress in the UU tests.

A comparison between the measured (undrained) values of $(\sigma_1\text{-}\sigma_3)_f$ obtained from the UU tests and the estimated (drained) value of $(\sigma_1\text{-}\sigma_3)_f$ using Equation (3) as a function of the initial suction is shown in Figure 8(c). The range of average undrained shear strength $(\sigma_1\text{-}\sigma_3)_{f,ave}$ values measured under the different axial strain rates is also shown in this figure. In order to calculate the effective confining stress (σ'_3) as part of the estimate of the drained shear strength in Equation (3), the suction stress (σ_s) estimated using Equation (6) was subtracted from the applied net stress (σ_{net}) following Equation (5). The drained friction angle (ϕ') was assumed to be constant with suction for this calculation. Similar to the shape of the SSCC, the suction has the greatest effect on the drained value of $(\sigma_1\text{-}\sigma_3)_f$ at intermediate suction values near or above the air entry suction but below the suction at the inflection point of the SWRC. This indicates that the initial suction should not play a significant role in the shear strength of soils under high suctions due to the lower availability of water in the pores to hold the particles together via capillarity or adhesion. Several interesting conclusions can be drawn when comparing the values of $(\sigma_1\text{-}\sigma_3)_f$ for drained and undrained conditions. The values of $(\sigma_1\text{-}\sigma_3)_f$ from the UU tests are lower than those expected in drained conditions for the specimens compacted wet of optimum (compaction water contents of 17.6 and 19.3%). As the degree of saturation in these tests is 0.9 or greater, it is likely that the pore water phase is continuous throughout the soil specimens and the pore air phase is occluded. In this case, the comparison between the values of $(\sigma_1\text{-}\sigma_3)_f$ for drained and undrained conditions indicates that positive excess pore water and pore air pressures were likely generated during undrained shear, leading to a reduction in effective stress and potentially a reduction in suction. This explanation of the behavior at low initial suctions is consistent with the observations of Svoboda and McCartney (2014), who measured positive excess pore water pressures during CU tests on Boulder clay regardless of the initial suction value. However, the values of $(\sigma_1\text{-}\sigma_3)_f$ from the UU tests are greater than those in drained conditions for the specimens compacted dry of optimum (compaction water contents of 11.5 and 13.5%). At these lower initial degrees of saturation (approximately 0.6 to 0.7), it is likely that the pore air phase is continuous throughout the specimen and the pore water phase is occluded. Although it is possible that negative excess pore water pressures could be generated in drier conditions leading to an increase in effective stress, it is more likely that positive pore air pressure would be generated due to the compression of air voids leading to a decrease in effective stress. Accordingly, it is believed that the difference in $(\sigma_1\text{-}\sigma_3)_f$ for the specimens compacted wet of optimum (low suctions) and dry of optimum (high suctions) is due to dispersed or flocculated soil structures (Mitchell et al. 1965). However, the greater values of $(\sigma_1\text{-}\sigma_3)_f$ for the specimens compacted at a water content of 13.5% than those compacted at a water content of 11.5% is due to the impact of initial suction, as suction still has an impact on the drained shear strength at this range of suction values. Accordingly, the similar trends between the measured (undrained) and the estimated (drained) shear strength with suction can be expected regardless of the impact of compacting wet or dry of optimum.

CONCLUSIONS

Unconsolidated undrained (UU) triaxial tests were performed at increased loading rates to investigate the effects of strain rate on the undrained shear strength quantified using the maximum principal stress difference $(\sigma_1\text{-}\sigma_3)_f$ of a low plasticity clay at different initial compaction water contents. The following specific conclusions can be drawn from this study:

- The value of $(\sigma_1\text{-}\sigma_3)_f$ for compacted Boulder clay increases by approximately 4.1 to 9.7% per log cycle of axial strain rate, with a greater rate for specimens that are compacted dry of optimum.
- The increase in undrained shear strength with increasing strain rate can be associated with less excess pore air or pore water pressure during shearing at faster rates. A corresponding increase in secant modulus with strain rate indicates that specimens sheared at faster rates should undergo less deformation than the one that contributes to excess pore water pressure generation.

- The rate effects were observed to be similar regardless of the initial degree of saturation, indicating that although the excess pore air and pore water pressures at different initial degrees of saturation may differ they offset and have the same net effect on the effective stress state.
- Clays compacted at or above the line of optimums are expected to experience positive excess pore water pressure generation during shear similar to the saturated soils under the same stress state, and have lower undrained shear strength than drained shear strength.
- Clays compacted below the line of optimums are also expected to experience positive excess pore water pressure generation during shear similar to saturated soils under the same stress state, but will have a greater undrained shear strength than drained shear strength due to flocculated conditions associated with compaction.
- If the compaction effects on the soil structure are neglected, the trends in undrained shear strength with initial suction are similar to trends in drained shear strength with initial suction.

ACKNOWLEDGMENTS

Funding for this research was provided by Office of Naval Research (ONR) grant N00014-11-1-0691. Special thanks are given to Alexandra Wayllace, Yi Dong, and Ning Lu at Colorado School of Mines for measuring the soil-water retention curve for Boulder clay. The opinions in this paper are those of the authors alone.

APPENDIX I. REFERENCES

Abramento, M. and Carvalho, C.S. (1989). “Geotechnical parameters for the study of natural slopes instabilization at ‘Serra do Mar’, Brazil.” Proceedings of the International Conference on Soil Mechanics and Foundation Engineering. A.A. Balkema, Rotterdam, Netherlands, Rio de Janeiro, Brazil, 1599-1602.

ASTM D2850. (2007) Standard Test Method for Unconsolidated-Undrained Triaxial Compression Test on Cohesive Soils. ASTM International. West Conshohocken, PA.

Bishop, A.W. (1959). “The principle of effective stress.” Teknisk Ukeblad I Samarbeide Med Teknikk. Oslo, Norway. 106(39), 859-863.

Bishop, A.W. and Donald, I.B. (1961). “The experimental study of partially saturated soil in the triaxial test.” Proc. 5th Int. Conference on Soil Mechanics and Foundation Engineering. 13-21.

Bolzon, G., and Schrefler, B.A. (1995). “State surfaces of partially saturated soils: an effective pressure approach.” Applied Mechanics Reviews. 48(10), 643-649.

Casagrande, A. and Shannon, W.L. (1948). “Stress-deformation and strength characteristics of soils under dynamic loads.” Proc. 2nd ICSMFE. Volume V. Rotterdam, Netherlands. 29-34.

Cetin, H. and Gökoğlu, A. (2013). “Soil structure changes during drained and undrained triaxial shear of a clayey soil.” Soils and Foundations. 53(5), 628-638.

Crawford, C.B. (1959). “The influence of rate of strain on effective stresses in sensitive clay.” Symposium on Time Rates of Loading in Soil Testing. STP 254. ASTM International, West Conshohocken, PA. 36-48

Cunningham, M.R., Ridley, A.M., Dineen, K., and Burland, J.B. (2003). “The mechanical behaviour of a reconstituted unsaturated silty clay. Géotechnique. 53(2), 183-194.

Escario, V. and Saez, J. (1986). “The shear strength of partly saturated soils.” Géotechnique. 36(3), 453-456.

Feuerharmel, C., Bica, A.V.D., Gehling, W.Y.Y., and Flores, J.A. (2005). “A study of the shear strength of two unsaturated colluvium soils.” In: Tarantino, A., Romero, E., Cui, Y.J. (Eds.), Proceedings of the International Symposium on Advanced Experimental Unsaturated Soil Mechanics. Taylor & Francis, Trento, Italy, 169-174.

Fredlund, D.G., Morgenstern, N.R., and Widger, R.A. (1978). “Shear strength of unsaturated soils.” Canadian Geotechnical Journal 15 (3), 313-321.

Fredlund, D.G., Rahardjo, H., and Gan, J.K.M. (1987). “Non-linearity of strength envelope for unsaturated soils.” Proceedings of 6th International Conference on Expansive Soils, New Delhi, India, 49-54.

Fredlund, D.G., and Rahardjo, H. (1993). Soil Mechanics for Unsaturated Soils. John Wiley & Sons, NY.

Gan, J.K.M., Fredlund, D.G., and Rahardjo, H. (1988). “Determination of the shear strength parameters of an unsaturated soil using the direct shear test.” Canadian Geotechnical Journal 25(3), 500-510.

Graham, J., Crooks, J.H.A., and Bell, A.L. (1983). “Time effects on the stress-strain behaviour of soft natural clays.” Géotechnique. 33(3), 327-340.

Hilf, J.W. (1948). “Estimating construction pore pressures in rolled earth dams.” Proc. 2nd Int. Conference on Soil Mechanics and Foundation Engineering. Rotterdam, Vol. 3, 230-240.

Ho, D.Y.F., and Fredlund, D.G. (1982). “A multistage triaxial test for unsaturated soils.” Geotechnical Testing Journal 5 (1/2), 18-25.

Lefebvre, G. and LeBoeuf, D. (1987). “Rate effects and cyclic loading of sensitive clays.” Journal of Geotechnical Engineering. 113(5), 476-489.

Lew, K.V. (1981). Yielding Criteria and Limit State in a Winnipeg Clay. MS Thesis. University of Manitoba.

Lu, N., and Likos, W.J. (2006) “Suction stress characteristic curve for unsaturated soil.” Journal of Geotechnical Geoenvironmental Engineering. 132(2), 131-142.

Wayllace A., and Lu, N. (2012). “A transient water release and imbibitions method for rapidly measuring wetting and drying soil water retention and hydraulic conductivity functions.” Geotechnical Testing Journal. 35(1), 103-117.

Lu, N., Godt, J., and Wu, D. (2010). “A closed form equation for effective stress in variably saturated soil.” Water Resources Research. 46(5), W05515.

Mitchell, J.K., Hooper, D.R. and Campanella, R.G. (1965). “Permeability of compacted clay.” Journal of the Soil Mechanics and Foundation Division. 91(SM4), 41-65.

Mun, W., and McCartney, J.S. (2015). “Compression mechanisms of unsaturated clay under high stress levels.” Canadian Geotechnical Journal. 52, 10.1139/cgj-2014-0438.

Nakase, A., and Kamei, T. (1986). “Influence of strain rate on undrained shear characteristics of Ko-consolidated cohesive soils.” Soils and Foundations. 26(1), 85-95.

Nam, S., Gutierrez, M., Diplas, P., and Petrie, J. (2011). “Determination of the shear strength of unsaturated soils using the multistage direct shear test.” Eng. Geol., 122(3-4), 272-280.

Olson, R.E., and Langfelder, L.J. (1965). Pore-water pressures in unsaturated soils. J. Soil Mech. Found. ASCE. 91(SM4), 127-160.

Olson, R.E. and Parola, J.F. (1967). “Dynamic shearing properties of compacted clay.” International Symposium on Wave Properties and Dynamic Properties of Earth Materials. ASCE. 173-182.

Penumadu, D., Skandarajah, A. and Chameau, J.L. (1998). “Strain-rate effects in pressuremeter testing using a cuboidal shear device: experiments and modeling.” Canadian Geotechnical Journal. 35(1), 27-42.

Rahardjo, H. (1990). The Study of Undrained and Drained Behavior of Unsaturated Soils. Ph.D. thesis, Department of Civil Engineering, University of Saskatchewan, Saskatoon, Saskatchewan.

Rahardjo, H., Lim, T.T., Chang, M.F., and Fredlund, D.G. (1995). “Shear-strength characteristics of a residual soil.” Canadian Geotechnical Journal 32 (1), 60-77.

Rassam, D.W., and Williams, D.J. (1999). “A relationship describing the shear strength of unsaturated soils.” Canadian Geotechnical Journal, 36(2), 363-368

Richardson, A.M. and Whitman, R.V. (1963). “Effect of strain-rate upon undrained shear resistance of a saturated remolded fat clay.” Géotechnique. 13(4), 310-324.

Schlue, B.F., Moerz, T. and Kreiter, S. (2010). “Influence of shear rate on undrained vane shear strength of organic harbor mud.” Journal of Geotechnical and Geoenvironmental Engineering. 136(10), 1437-1447.

Seed, H.B., Chan, C.K., (1959). “Structure and strength characteristics of compacted clays.” Journal of the Soil Mechanics and Foundation Division. ASCE, 85(SM5), 87-128.

Soga, K. and Mitchell, J.K. (1996). “Rate-dependent undrained shear behavior of structured natural clays.” Proc., 1996 ASCE National Convention. ASCE, New York. 243-257.

Svoboda, J. and McCartney, J.S. (2013). “Shearing rate effects on dense sand and compacted clay.” Chapter 47 in Dynamic Behavior of Materials. Vol. 1. B. Song, ed. Springer, Vienna. 389-395.

Svoboda, J. and McCartney, J.S. (2014). “Impact of strain rate on the shear strength and pore water pressure generation in unsaturated clay.” Proceedings of GeoCongress 2014 (GSP 234). M. Abu-Farsakh and L. Hoyos, eds. ASCE. 1453-1462.

Vanapalli, S.K., Fredlund, D.G., Pufahl, D.E. and Clifton, A.W. (1996). “Model for the prediction of shear strength with respect to soil suction.” Canadian Geotechnical Journal 33(3), 379-392.

Vanapalli, S.K., Pufahl, D.E., and Fredlund, D.G. (1999). “The effect of soil structure and stress history on the soil-water characteristics of a compacted till.” Géotechnique. London, 49(2), 143-159.

Vanapalli, S.K. and Fredlund, D.G. (2000). “Comparison of different procedures to predict unsaturated soil shear strength.” Advances in Unsaturated Geotechnics. Geotechnical Special Publication, No.99. ASCE, Denver, CO, 195-209.

van Genuchten, M.T. (1980). “A closed-form equation for predicting the hydraulic conductivity of unsaturated soils.” Soil Science Society of America Journal. 44(5), 892-898.

Vaid, Y.P. and Campanella, R.G. (1977). “Time dependent behavior of undisturbed clay.” Journal of Geotechnical Engineering. 103(7), 693-709.

Vilar, O.M. (2006). “A simplified procedure to estimate the shear strength envelope of unsaturated soils.” Canadian Geotechnical Journal. 43(10), 1088-1095.

Zhu, J. and Yin, J. (2000). “Strain-rate-dependent stress strain behavior of over-consolidated Hong Kong marine clay.” Canadian Geotechnical Journal. 37(6), 1272-1282.

LIST OF TABLE AND FIGURE CAPTIONS

Table 1: Summary of strain rate effects on undrained shear strength of cohesive soils

Table 2: Properties of Boulder clay

Table 3: Initial specimen information for UU tests on Boulder clay

Table 4: Summary of UU test results

Table 5: Summary of the input values for the application of Hilf's analysis (1948)

Fig. 1: Boulder clay properties: (a) Standard Proctor compaction curve with initial compaction conditions of tested specimens; (b) Evaluation of typical initial suction values in compacted specimens; (c) Wetting- and drying-path soil water retention curves along with the

Fig. 2: Results from UU triaxial compression tests on compacted clay with different gravimetric water contents but the same initial void ratio of 0.52 (Each curve is an average of 3 curves): (a) w=11.5%; (b) w=13.5%; (c) w=17.6%; (d) w=19.3%

Fig. 3: (a) Principal stress difference at failure for specimens having different initial water contents plotted as a function of axial strain rate; (b) Strains at failure as a function of different axial strain rates

Fig. 4: Trends in the log-linear slope of the undrained shear strength vs. axial strain rate: (a) Impact of initial degree of saturation $S_{r,i}$; (b) Impact of initial ψ_i

Fig. 5: Axial strain rate effects on the principal stress difference at failure for compacted clay specimens having different: (a) Initial degrees of saturation $S_{r,i}$; (b) Initial suction ψ_i values

Fig. 6: Impact of axial strain rate on the secant modulus

Fig. 7: Strain rate effects on the secant modulus of compacted clay specimens having different: (a) Initial degrees of saturation $S_{r,i}$; (b) initial suction ψ_i values

Fig. 8: (a) Suction stress characteristic curve for Boulder clay estimated from the drying path SWRC; (b) Predicted pore air pressure development for Boulder clay during total stress application using the analysis of Hilf (1948); (c) Comparison between all values of $(\sigma_1\text{-}\sigma_3)_f$ measured in the UU triaxial compression tests with those expected in drained triaxial compression tests

Table 1: Summary of strain rate effects on undrained shear strength of cohesive soils

Reference	Soil description	Ave. LL	Ave. PI	Specimen type and stress history	Shearing approach	Specimen height (mm)	Max. axial strain rate (%/min) or min. time to "failure" (s)	Approx. % increase in undrained shear strength per log cycle of axial strain rate
Casagrande & Shannon (1948)	Saturated Cambridge clay (CL)	41	19	Intact and remolded, NC	Stress (fast) and strain (slow) controlled	90	0.01 s	15.0
Casagrande & Shannon (1948)	Saturated Boston clay (CL)	42	22	Intact and remolded, NC	Stress (fast) and strain (slow) controlled	90	0.1 s	13.0
Casagrande & Shannon (1948)	Saturated Stockton clay (CH)	62	40	Intact and remolded, OC	Stress (fast) and strain (slow) controlled	90	0.1 s	8.0
Richardson & Whitman (1963)	Saturated Mississippi River Clay (CH)	62	38	Remolded, NC and OC	Strain controlled with PWP	80	1 %/min	3.7
Olson & Parola (1967)	Unsaturated Goose Lake clay (CL)	31	14	Compacted	Stress (fast) and strain (slow) controlled	76	0.002-1s (fast) 1s – 100min (slow)	σ_3=690 kPa: 5.7-23.8 (fast), 1.3-5.4 (slow); σ_3=6900 kPa: 13.3-27.6 (fast), 1.4-8.2 (slow)
Vaid & Campanella (1977)	Saturated Haney clay (CL)	44	18	Intact, NC	Strain controlled with PWP	NR	10 %/min	7.0
Lew (1981)	Winnipeg clay (CH)	80	56	Intact, OC	Strain controlled with PWP	152	0.167 %/min	11.0-12.0
Graham et al. (1983)	Saturated Belfast clay (CH)	93	60	Intact, OC	Strain controlled with PWP	NR	0. 167 %/min	9.7-13.4
Nakase et al. (1986)	Saturated sand-clay mixtures (M30 - CH)	55	29	Remolded, anisotropic	Strain controlled with PWP	NR	0.7 %/min	10.6
Nakase et al. (1986)	Saturated sand-clay mixtures (M15 – CL)	35	15	Remolded, anisotropic	Strain controlled with PWP	NR	0.7 %/min	6.5
Nakase et al. (1986)	Saturated sand-clay mixtures (M10 – CL)	28	11	Remolded, anisotropic	Strain controlled with pore water pressure	NR	0.7 %/min	5.0
Lefebvre & LeBoeuf (1987)	Saturated Grande Baleine clay (CL)	34	12	Intact, isotropic, anisotropic	Stress (fast) and strain (slow) controlled	71	100 %/min	7.0-9.0
Lefebvre & LeBoeuf (1987)	Saturated Olga clay (CH)	68	40	Intact, isotropic, anisotropic	Stress (fast) and strain (slow) controlled	71	100 %/min	12.0-13.0
Penumadu et al. (1998)	Saturated Kaolin (CH)	63	30	Remolded, NC	Strain controlled with PWP	102	5 %/min	14.3
Penumadu et al. (1998)	Saturated Kaolin-silica mix (CH)	63	30	Remolded, NC	Strain controlled with PWP	102	5 %/min	15.3
Zhu & Yin (2000)	Saturated Hong Kong Marine clay (CH)	60	32	Remolded, NC and OC	Strain controlled with PWP	100	0.25 %/min	3.0-6.0
Svoboda & McCartney (2014)	Compacted Boulder clay (CL)	43	22	Compacted	Strain controlled with PWP	142	14.5 %/min	14.1 (saturated) 6.2-15.2 (unsaturated)

Table 2: Properties of Boulder clay

Property	Value	Units
D_{10}	< 1.7×10^{-4}	mm
D_{30}	< 0.001	mm
D_{50}	0.001	mm
Percent fines	100	%
G_s	2.70	-
Liquid limit, LL	41	-
Plastic limit, PL	18	-
Plasticity index, PI	23	-
Activity, A	0.75	-
Maximum dry unit weight, $\gamma_{d,max}$	17.4	kN/m^3
Optimum water content, w_{opt}	17.5	%
Compression index, C_c	0.23	-
Recompression index, C_r	0.04	-
Drained friction angle, ϕ'	34	°

Table 3: Initial specimen information for UU tests on Boulder clay

Axial strain rate (%/min)	Compaction gravimetric water content, w_{ave} (%)	Initial dry density, $\gamma_{d,ave}$ (kN/m^3)	Initial void ratio, $e_{i,ave}$	Initial degree of saturation, $S_{r,ave}$	Initial suction from tensiometer, ψ_{ini} (kPa)
0.1	11.5	17.39	0.52	0.59	120
1.5					
15.0					
150.0					
0.1	13.5	17.40	0.52	0.70	101
1.5					
15.0					
150.0					
0.1	17.6	17.39	0.52	0.91	80
1.5					
15.0					
150.0					
0.1	19.3	17.39	0.52	0.99	10
1.5					
15.0					
150.0					

Table 4: Summary of UU test results

Average grav. water content (%)	**Axial strain rate (%/min)**	**Test no. 1 $(\sigma_1-\sigma_3)_f$ (kPa)**	**Test no. 2 $(\sigma_1-\sigma_3)_f$ (kPa)**	**Test no. 3 $(\sigma_1-\sigma_3)_f$ (kPa)**	**Average $(\sigma_1-\sigma_3)_f$ (kPa)**	**Standard deviation $(\sigma_1-\sigma_3)_f$ (kPa)**	**A (kPa/ %/min)**	**% increase in $(\sigma_1-\sigma_3)_f$ per log cycle of axial strain rate**
11.5	0.1	1018	1073	1056	1049	28.16	18.83	9.7
	1.5	1072	1114	1109	1099	22.80		
	15.0	1122	1154	1174	1150	26.07		
	150.0	1200	1171	1182	1184	14.61		
13.5	0.1	926	875	879	893	28.66	18.38	7.7
	1.5	952	924	914	930	19.70		
	15.0	959	982	948	963	17.04		
	150.0	1045	1026	1025	1032	11.09		
17.6	0.1	441	449	425	438	12.06	14.75	4.9
	1.5	451	462	474	462	11.94		
	15.0	489	513	501	501	12.25		
	150.0	537	554	545	545	8.36		
19.3	0.1	314	294	273	294	20.23	12.20	4.1
	1.5	307	297	323	309	13.24		
	15.0	348	329	328	335	10.99		
	150.0	394	379	381	385	8.52		

Table 5: Summary of the input values for the analysis of Hilf (1948)

Initial degree of saturation, $S_{r,0}$	**Initial porosity, n_0**	**Average coefficient of volume compressibility, m_v (1/kPa)**
0.59	0.34	3.00×10^{-5}
0.70	0.34	3.24×10^{-5}
0.91	0.34	1.38×10^{-5}

Figure 1

Click here to download high resolution image

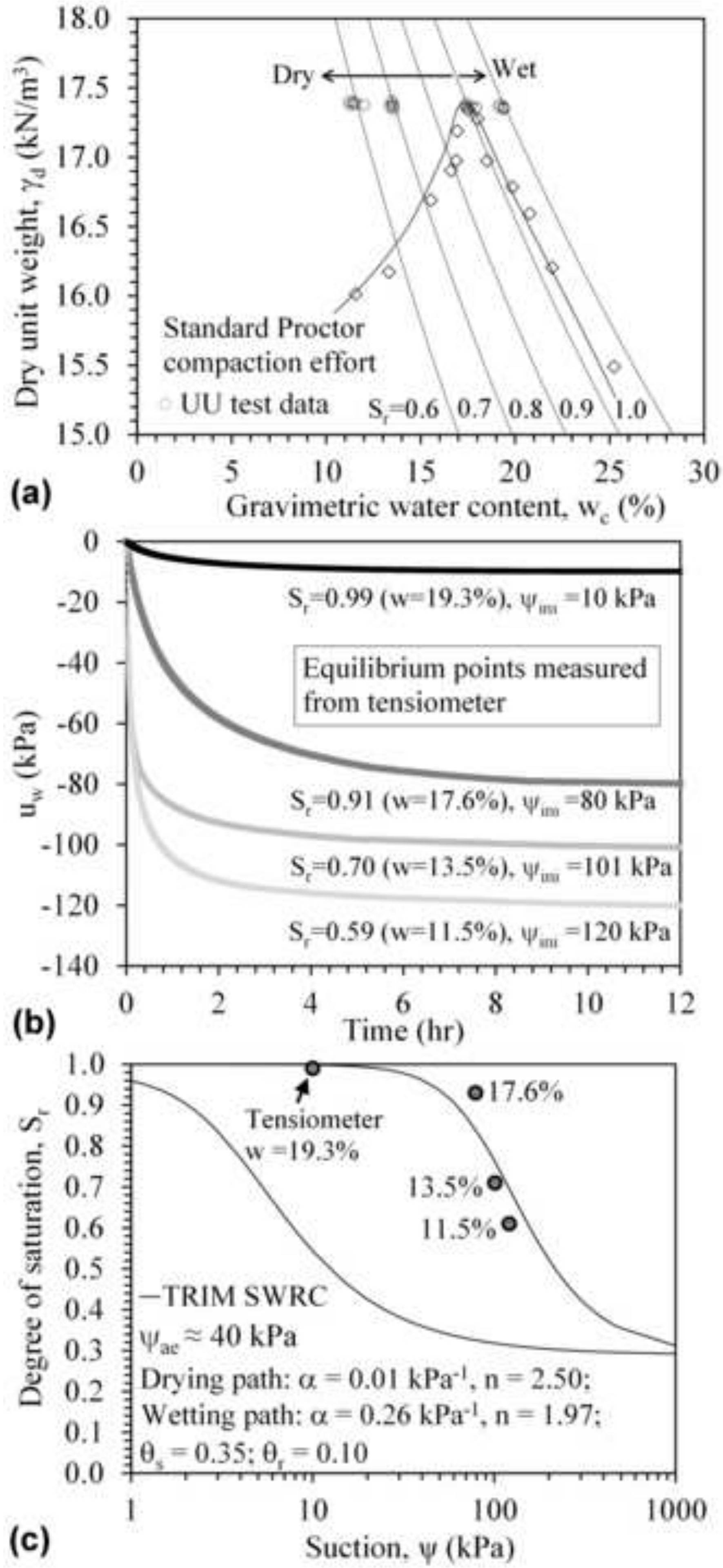

Figure 2

Click here to download high resolution image

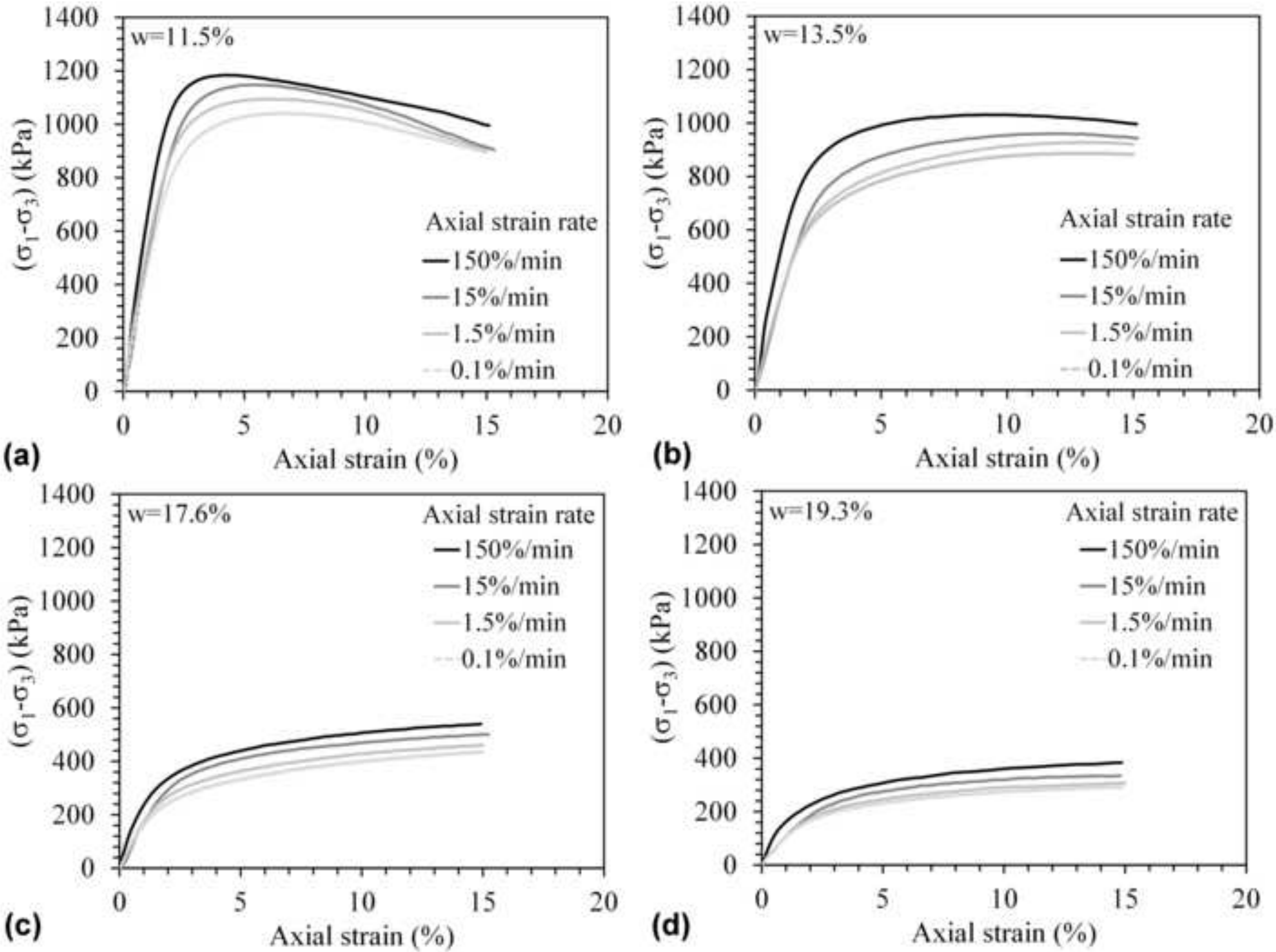

Figure 3

Click here to download high resolution image

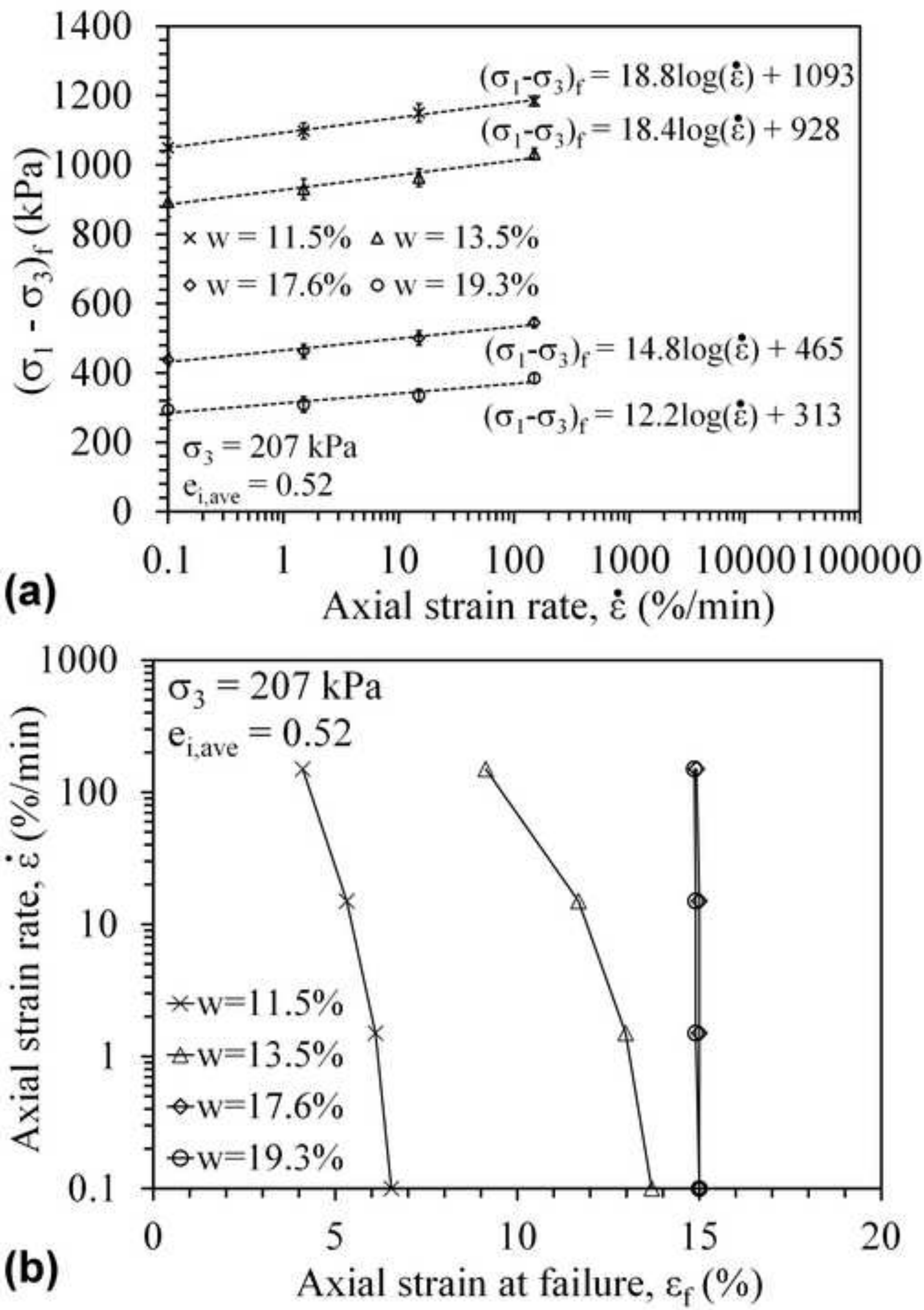

Figure 4

Click here to download high resolution image

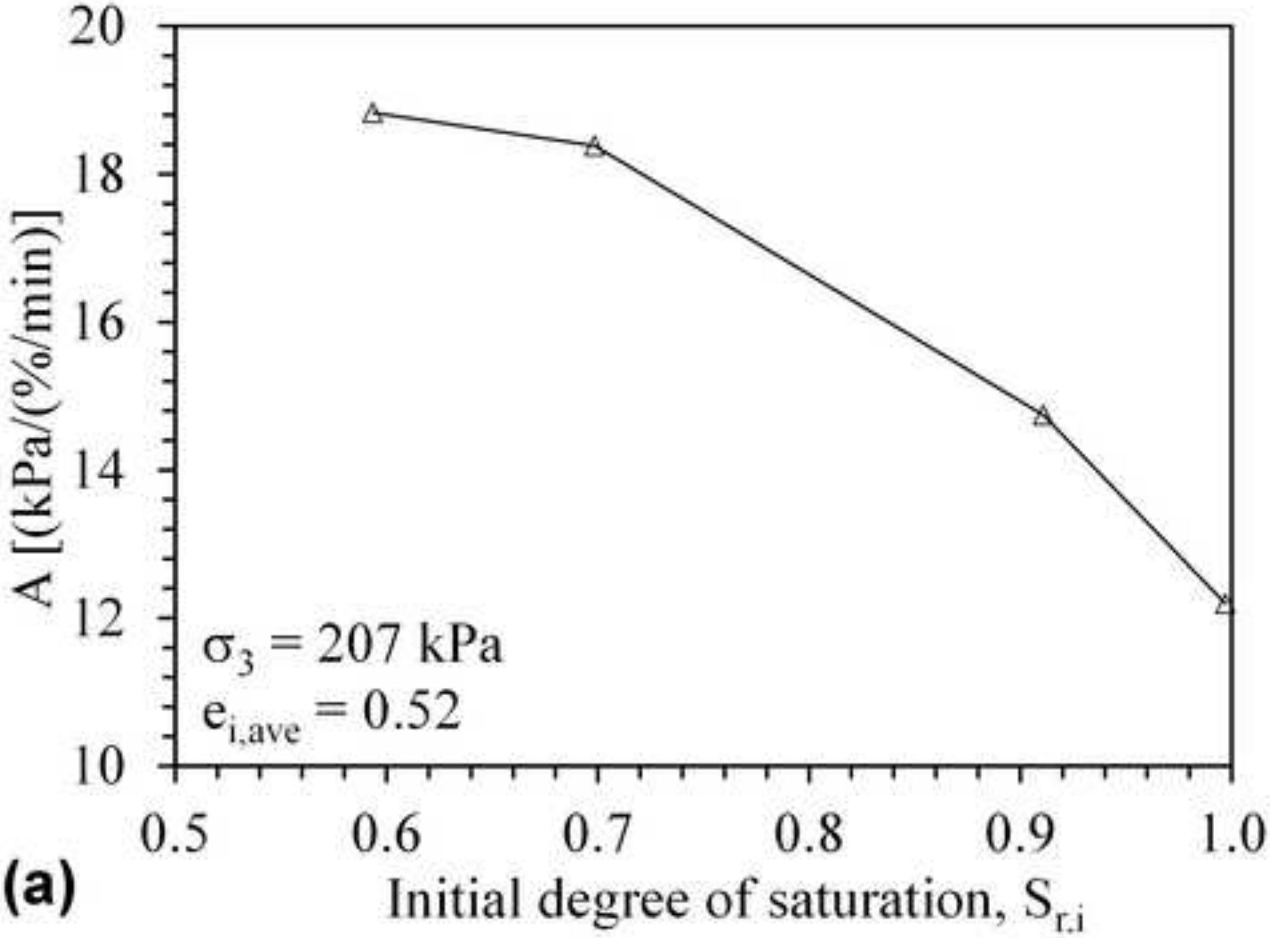

(a)

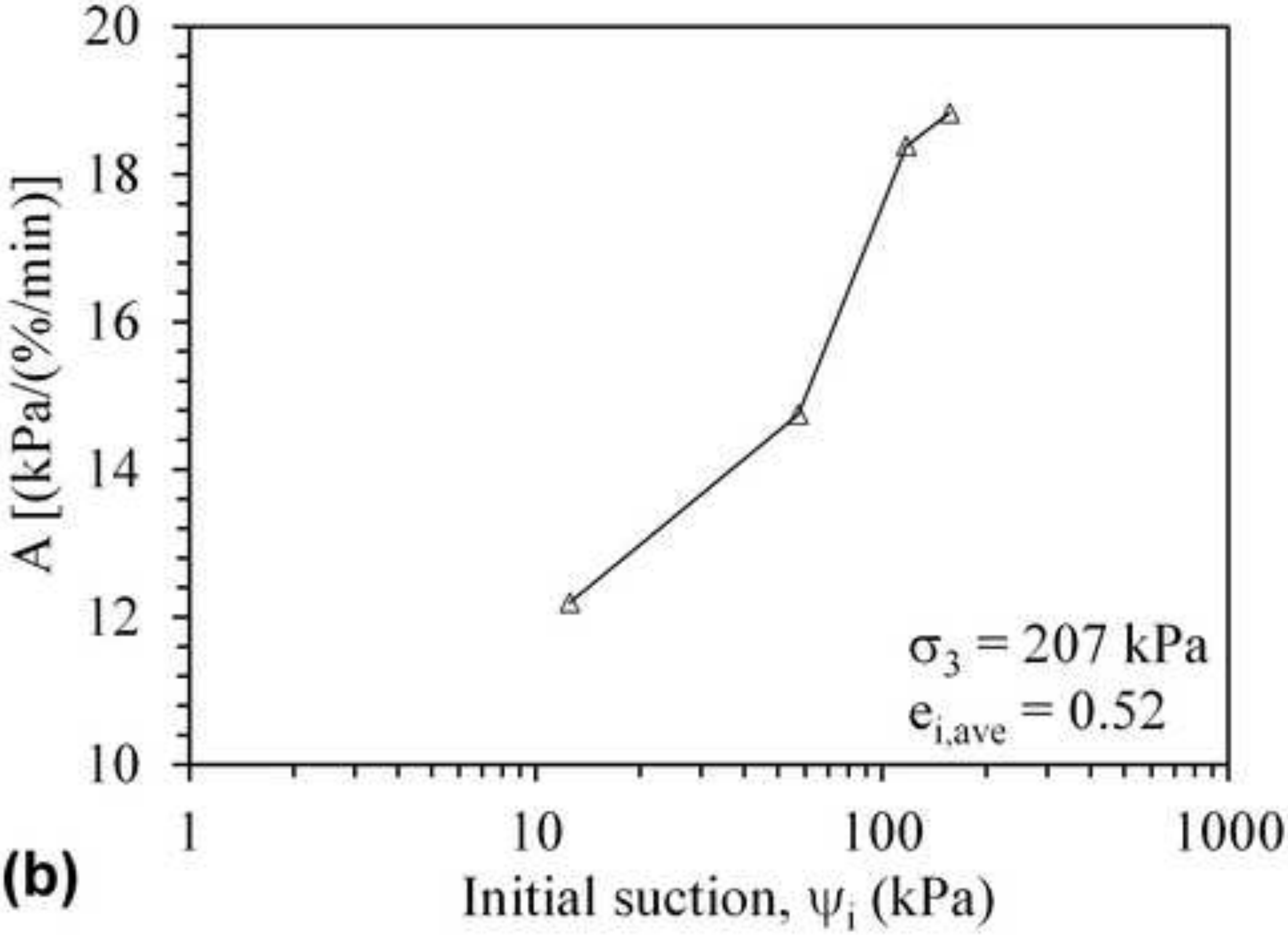

(b)

Figure 5
Click here to download high resolution image

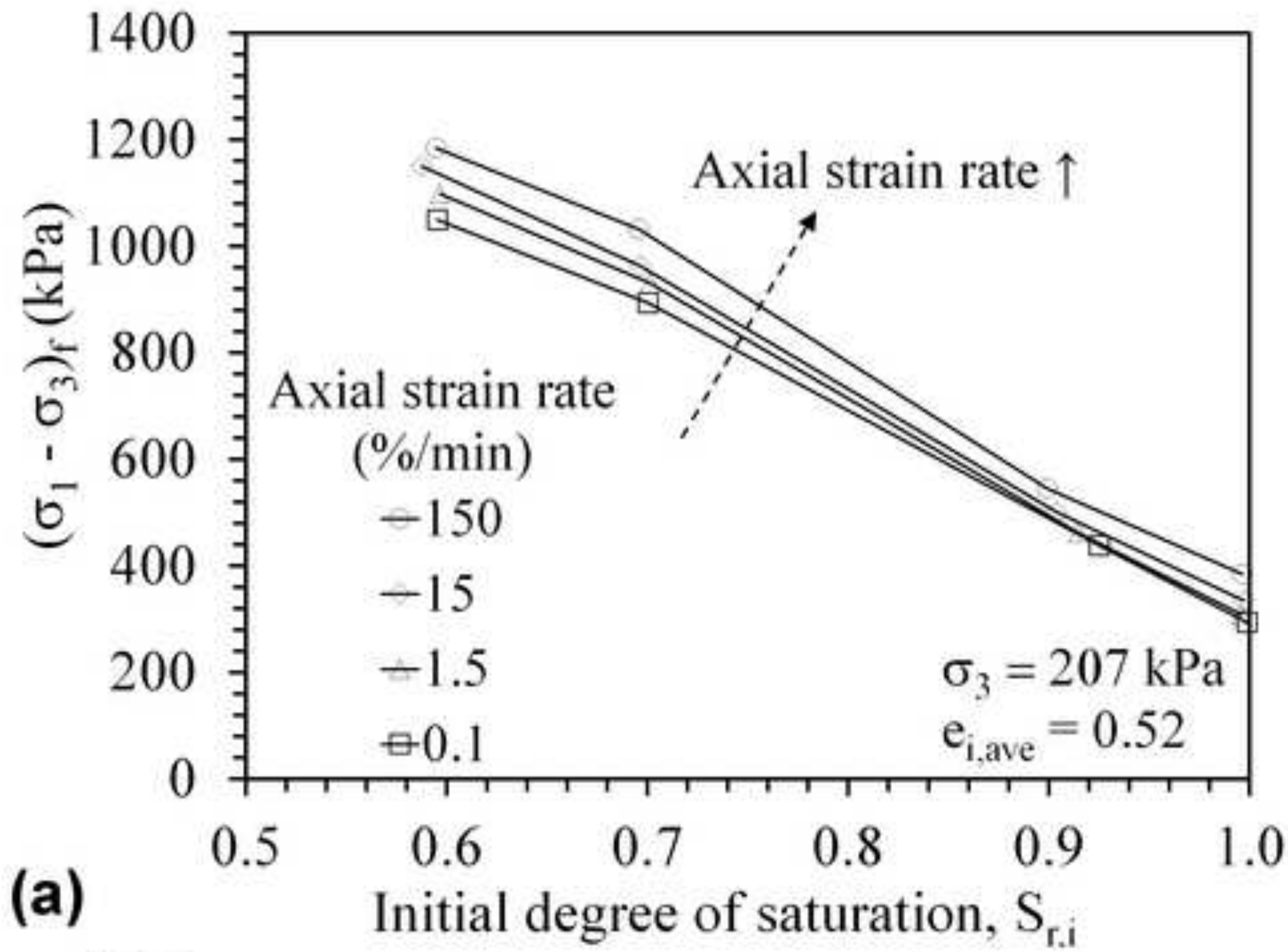

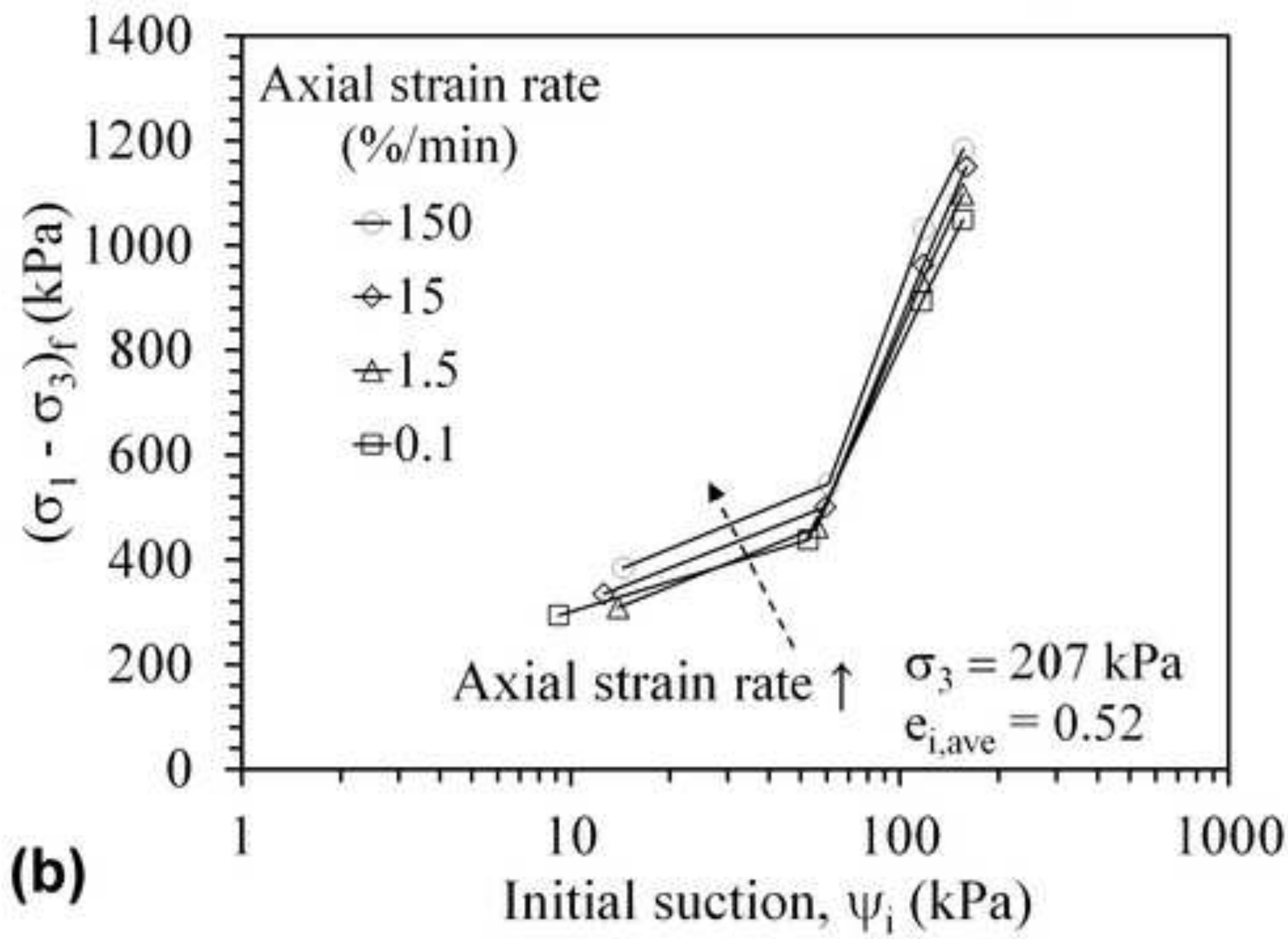

Figure 6

Click here to download high resolution image

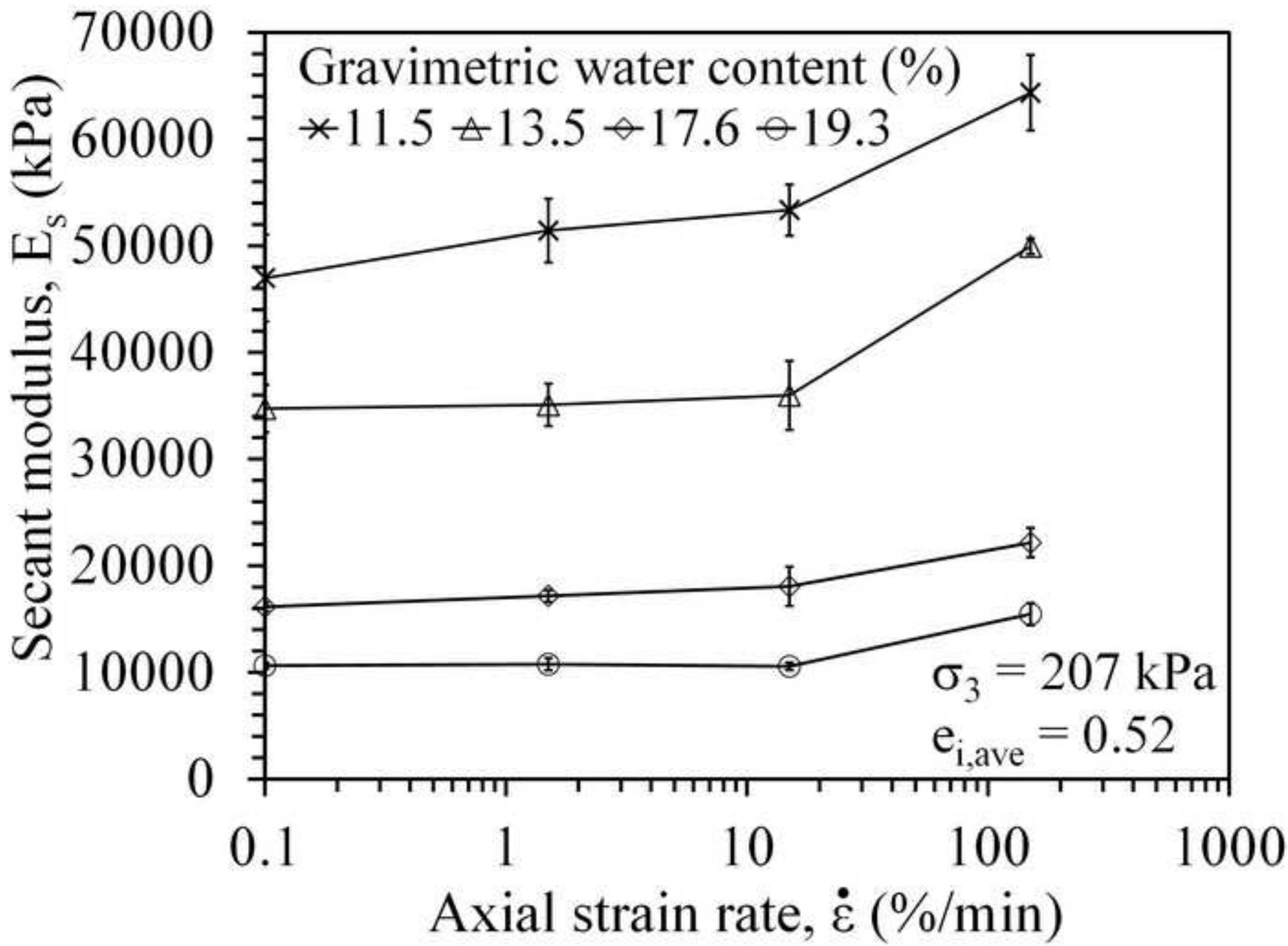

Figure 7
Click here to download high resolution image

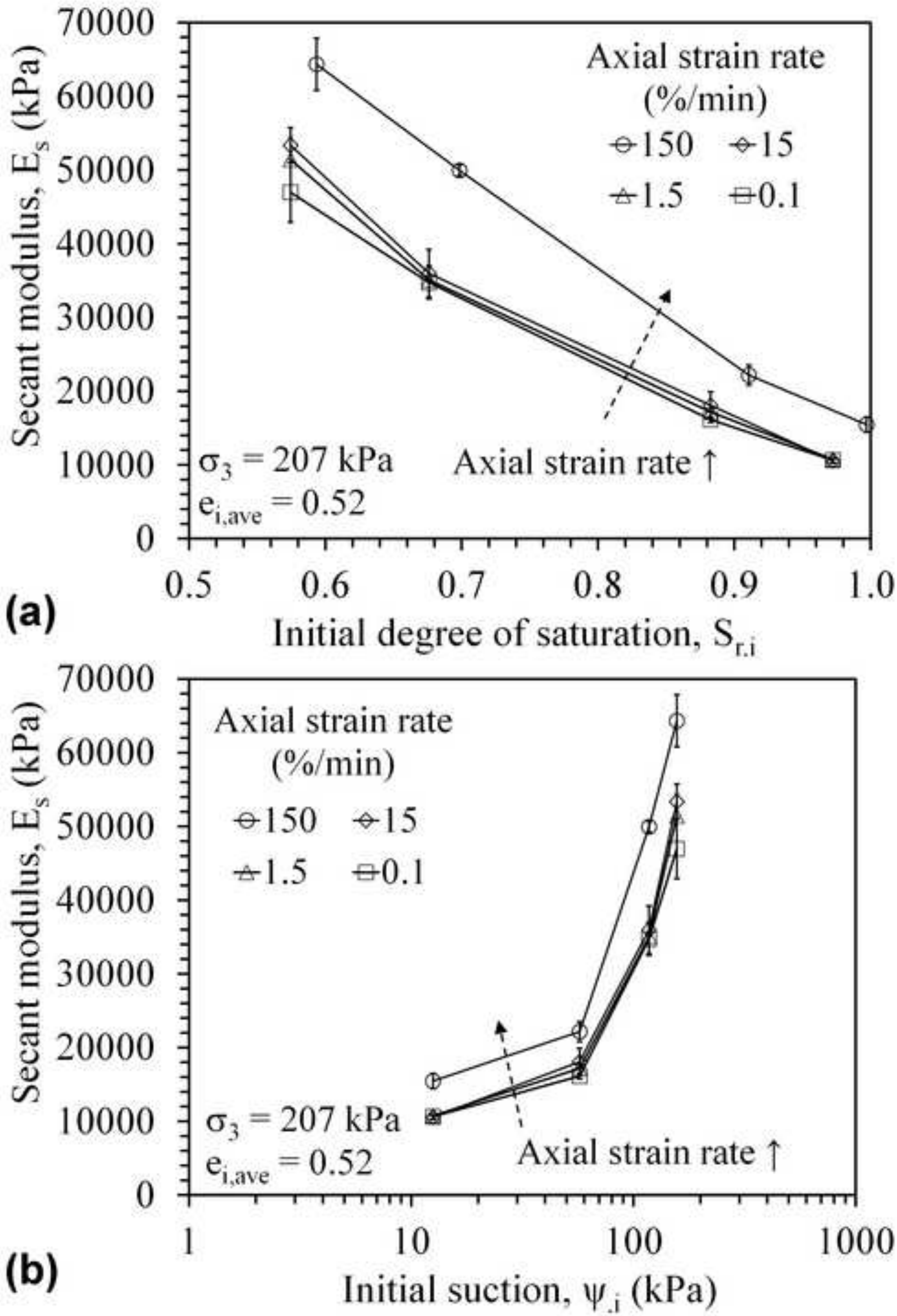

Figure 8
Click here to download high resolution image